ACS OMEGA

http://pubs.acs.org/journal/acsodf

Article

Plasmonic-Based Biosensor for the Early Diagnosis of Prostate Cancer

Thakshila Liyanage, Bayan Alharbi, Linh Quan, Aurora Esquela-Kerscher, and Gymama Slaughter*

Cite This: *ACS Omega* 2022, 7, 2411−2418

Read Online

ACCESS | Metrics & More | Article Recommendations

ABSTRACT: A tapered optical fiber (TOF) plasmonic biosensor was fabricated and used for the sensitive detection of a panel of microRNAs (miRNAs) in human serum obtained from noncancer and prostate cancer (PCa) patients. Oncogenic and tumor suppressor miRNAs *let-7a*, *let-7c*, miR-200b, miR-141, and miR-21 were tested as predictive cancer biomarkers since multianalyte detection minimizes false-positive and false-negative rates and establishes a strong foundation for early PCa diagnosis. The biosensing platform integrates metallic gold triangular nanoprisms (AuTNPs) laminated on the TOF to excite surface plasmon waves in the supporting metallic layer and enhance the evanescent mode of the fiber surface. This sensitive TOF plasmonic biosensor as a point-of-care (POC) cancer diagnostic tool enabled the detection of the panel of miRNAs in seven patient serums without any RNA extraction or sample amplification. The TOF plasmonic biosensor could detect miRNAs in human serum with a limit of detection between 179 and 580 aM and excellent selectivity. Statistical studies were obtained to differentiate cancerous from noncancerous samples with a *p*-value <0.0001. This high-throughput TOF plasmonic biosensor has the potential to expand and advance POC diagnostics for the early diagnosis of cancer.

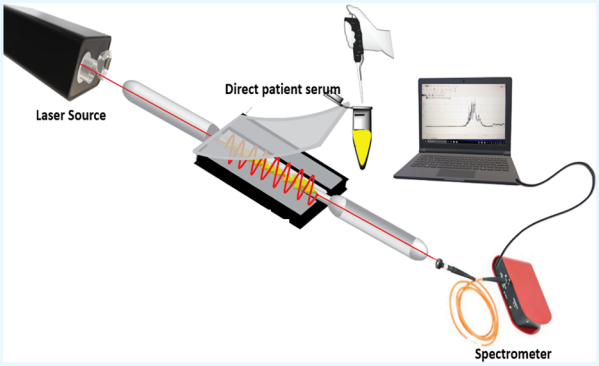

1. INTRODUCTION

Cancer is the second leading cause of death globally, and it costs our nation too many lives and consumes resources. In 2018, 9.6 million people died from this disease.[1] Among all of the cancers, breast cancer and prostate cancer (PCa) are the two most diagnosed cancers in women and men, respectively. PCa is the second most frequent malignancy in men with over 1.3 million new cases and 358 989 deaths worldwide, thereby representing 3.8% of all deaths caused by cancer in men in 2018.[2] The majority of PCa is adenocarcinoma, which appears in the secretory epithelial cells of prostatic ducts.[3] Currently, a symptom-based approach is used to diagnose PCa followed by an identification blood test to detect the prostate-specific antigen (PSA) concentration level in the serum. When the PSA level exceeds the threshold concentration of 4 ng/mL, further investigation is necessitated via a digital rectal examination and tissue biopsy. These approaches are invasive, increase discomfort levels for patients, and can carry procedural risks.[4] However, the biggest burden associated with PSA screening is that two-thirds of positive PSA tests are in fact false positives due to the low specificity of the PSA biomarker for PCa and one-fifth of PSA testing results in false negatives, missing men with significant PCa disease. Although biomarker-based diagnostics continue to play an important role in the detection of cancer, biomarkers with high specificity to PCa have not been explored. Therefore, there is an unmet need for a noninvasive PCa test that can distinguish healthy vs. cancerous cells more specifically than PSA.

Early diagnosis using biomarkers specific to PCa can greatly enhance the PCa survival rate and minimize the cost associated with the overall treatment.[5,6] MicroRNAs (MiRNAs) as biomarkers have garnered significant attention because of the critical role they play in various physiological and pathological progresses, including carcinogenesis.[7−13] MiRNAs are small noncoding RNAs of ∼19 to 22 nucleotides in length, which are capable of modulating gene activity at the post-transcriptional level. MiRNAs are commonly dysregulated in tissues and fluids (i.e., serum) of cancer patients compared to normal populations, and these expression profiles closely correlate with disease aggressiveness, disease prognosis, and therapy response.[14] Functional studies indicate that aberrant miRNA expression directly impacts prostate tumorigenesis by targeting factors that control cell cycle progression, apoptosis, DNA repair, differentiation, androgen signaling, angiogenesis,

Received: November 17, 2021
Accepted: December 17, 2021
Published: January 5, 2022

https://doi.org/10.1021/acsomega.1c06479
ACS Omega 2022, 7, 2411−2418

Scheme 1. (A) Schematic Representation of the Fabricated Tapered Optical Fiber (TOF) Biosensing Platform. (B) Gold Triangular Nanoprisms (AuTNPs) Covalently Bonded to the TOF. (C) Immobilized Single-Stranded DNA (ssDNA) and Poly(ethylene Glycol)-Thiol (PEG-SH) as Bioreceptor and Spacer, Respectively. (D) Hybridization of Target miRNA to ssDNA in a Complex Serum Environment that Contains Other Endogenous Biomolecules

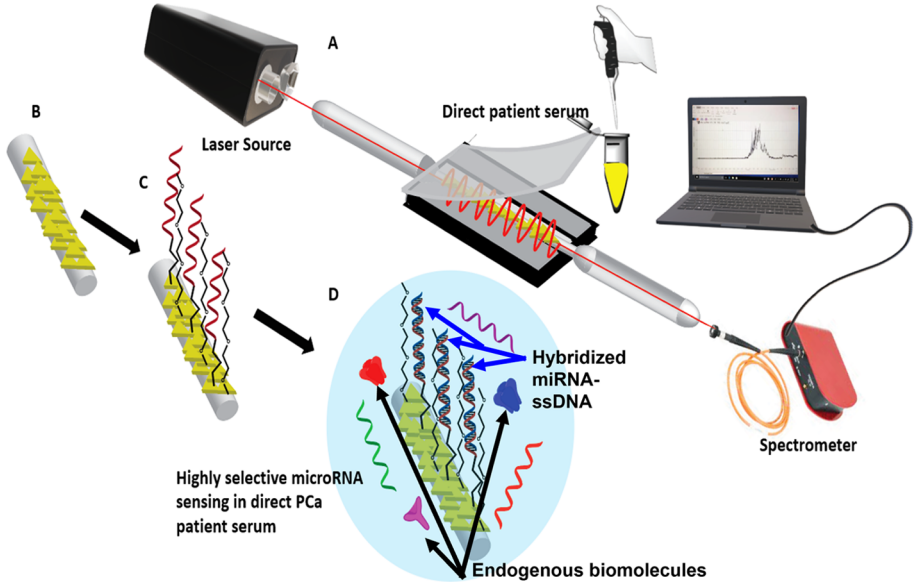

hypoxia, and chromatin remodeling. Oncogenic miRNAs are commonly overexpressed in PCa patients and promote cancer development by blocking tumor suppressor genes (i.e., TP53, PTEN). Similarly, prostate tumor suppressor miRNAs are underexpressed in cancer patients and act to inhibit malignant growth by targeting oncogenic factors and regulate cancer cell differentiation or apoptosis.[15,16] Mass-spectrometry imaging has gained significant attention for the development of label-free chemical imaging approaches in biological samples.[17−19] Laser desorption/ionization mass-spectrometry (LDI-MS)-based metabolic fingerprinting was recently explored for the diagnosis medulloblastoma, wherein the machine learning algorithm implemented correctly differentiated medulloblastoma patients from healthy controls using a panel of serum metabolite biomarkers.[18] Pei et al. demonstrated LDI-MS-based metabolic fingerprinting in successfully diagnosing gynecological cancers.[19] However, these techniques require sophisticated instrumentation and sample pretreatment prior to imaging and thus further limit point-of-care testing.

Different from LDI-MS, optical biosensors have been demonstrated to simplify the assay and enable the direct detection of nucleic acids.[20,21] Quantitative measurement of miRNAs has been achieved with microarrays and quantitative real-time polymerase chain reaction (qRT-PCR) technologies; however, these techniques are expensive and labor-intensive, requiring sample preparation and amplification steps.[22] Consequently, surface-enhanced Raman scattering (SERS) continues to garner significant attention as a powerful tool for measuring metabolites in biological fluids.[23,24] To enhance the performance of surface-enhanced Raman scattering (SERS)-based immunoassay, a linear support vector machine algorithm was demonstrated to successfully classify PCa, benign prostate hyperplasia (BPH), and healthy subjects using SERS-based immunoassay with an accuracy rate of 50% using serum PSA, and the classification performance increased to 70% when multiple tumor markers were used,[23] thereby illustrating the effectiveness of machine learning in analyzing multiple tumor biomarkers in serum and its potential application in point-of-care testing.

In our previous work, we reported on the successful fabrication of a tapered optical fiber (TOF) plasmonic biosensors for detection of a panel of prostate tumor suppressor and oncogenic miRNAs (let-7a, let-7c, miR-141, miR-21, miR-200b) diluted in standard buffered solution. Since TOFs are very sensitive to changes in the surrounding refractive index and the input light wavelength, we employed highly sensitive metallic nanostructure laminated on the TOF region to enhance the evanescent field to make the biosensor more sensitive to the local surface plasmon waves.[25] Herein, we report the improved use of TOF plasmonic biosensors to achieve highly sensitive and specific detection of miRNAs in PCa patient biological fluids (serum) while mitigating nonspecific binding for surface-based biosensors. Poly-(ethylene glycol)-thiol (PEG-SH) was used as a spacer molecule to minimize nonspecific adsorption of endogenous biomolecules and provided excellent antifouling effects. The use of the TOF plasmonic biosensor enabled the sensitive detection of a panel of miRNAs in seven patient serums representing noncancer, low-risk, and high-risk PCa, and expression profiling did not require RNA extraction or sample amplification. Expression profiles for let-7a and let-7c obtained by qRT-PCR correlated with the biosensor data. This work implicates the possibility of using TOF plasmonic biosensors for rapid and noninvasive diagnostic screening and early PCa detection using multianalyte detection of miRNAs biomarkers to minimize false-positive and false-negative rates and establish a strong foundation for early PCa diagnosis.

2. MATERIALS AND METHODS

2.1. Materials. Chloro(triethyl phosphine) gold (I) (Et3PAuCl, 97%), poly(methylhydrosiloxane) (PMHS, Mn = 1700−3300), and triethylamine (TEA, 98%) were procured from Sigma-Aldrich. ACS grade acetonitrile (CH3CN, 99.9%), ethanol (22 proof), and (3-mercaptopropyl)-trimethoxysilane

https://doi.org/10.1021/acsomega.1c06479
ACS Omega 2022, 7, 2411−2418

(MPTES, 94%) were procured from Thermo Scientific and used as received. Synthesized single-stranded DNA (ssDNAs) and miRNA oligonucleotides (hsa-*let-7a*, hsa-*let-7c*, hsa-miR-141-3p, hsa-miR-21-5p, hsa-miR-200b-3p) were procured from Integrated DNA Technologies.

2.2. Spectroscopy and Microscopy Characterizations. Absorption and extinction spectra in the range of 400−1000 nm were collected with a Spectra. Max M5 microplate reader from Molecular Devices, LLC. Extinction spectra of AuNPs, in the solution phase, were measured to determine the LSPR peak position (λ_{LSPR}). For the calibration study, all transmission spectra were obtained in phosphate-buffered saline (PBS) for all TOF using a Superk Compact supercontinuum lasers in the range of 450−2400 nm and a compact Czerny-Turner CCD spectrometer (CCS200, Thorlabs Inc.) as the laser source and detector, respectively, at room temperature. The resulting spectra were displayed on the computer for visualization.

2.3. Fabrication and Functionalized TOF. The tapered fiber was fabricated using a tapering rig system (Aerotech PR0115SL system) to form the TOF structure. Briefly, the middle section of a 1 m length single-mode fiber (SMF) was stripped of the polymer buffer coating material and cleaned with acetone prior to stretching through flame brushing technique and placed on the tapering rig system.[25] A butane flame was used to heat the fiber while pulling the fiber in the $x-y$ direction and oscillating the butane flame in the z-direction (5,10,15) for 30 s to achieve a constant waist diameter. The 3 cm region of the fabricated TOF was transitioned from a diameter of 125 μm to a taper waist diameter of ∼5 μm. The fabricated TOF was then carefully removed from the stage and mounted on a Teflon substrate that consisted of a 48 mm × 6 mm × 2 mm ($l \times w \times d$) cell to contain the analyte within the tapered region for surface functionalization and miRNA profiling (Scheme 1A). The substrate surface was sealed with poly(dimethylsiloxane) (PDMS) while exposing inlets and outlets.

2.4. Functionalization of TOF. The TOF was separately functionalized through two steps: MPTMS derivatization and gold triangular nanoprism (AuTNP) lamination. In the former step, TOFs were cleaned in a mixture of HCl/MeOH (1:1) followed by copious washing in DI water and dried in air for 3 h. The dried TOFs were immersed in 15% MPTMS−ethanol solution for 30 min followed by an ethanol rinse to remove unbound MPTMS from the TOF surface. In the later step, we synthesized AuTNPs by following previously published methods.16. Briefly, 10 mg of $Et_3PAu(I)Cl$ was dissolved in 40 mL of CH_3CN and stirred at medium speed for 5−10 min at room temperature. Then, 0.038 mL of TEA was added to the reaction mixture and heated gradually to 40 °C for 20 min. Then, 0.6 mL of PMHS was added to the solution and stirred for 3 h. The resulting solution was centrifuged at 4500 rpm for 40 min to remove the unreacted PMHS, and the obtained precipitation was redissolved in ultrapure water and analyzed using UV visible spectroscopy. The derivatized TOF was placed in 800 μL of AuTNPs for 1 h to laminate the TOF with Au nanostructures.

2.5. Biosensor Detection of miRNAs. The AuTNP-laminated TOFs were separately incubated in the respective 5 μM complementary ssDNA probe solution (ssDNA-HS-$(CH_2)_n$-X/SH (where X is the complementary base pairs for the target miRNA)) and 0.1 M tris(2-carboxyethyl) phosphine (TCEP) solution for 1 h to reduce disulfide to thiol. A 1 mM poly(ethylene glycol)-thiol (PEG-SH (1:1000)) solution was added and allowed to react overnight, followed by rinsing in PBS to remove any unbound reactants. The resulting ssDNA/PEG-functionalized TOF serves as the TOF plasmonic biosensor ready for the detection of target miRNA molecules from human serum samples.

2.6. Human Serum Samples. The deidentified human serum samples were obtained from the Eastern Virginia Medical School (EVMS) Biorepository under protocols was approved by the EVMS Institutional Review Board and in accordance with NIH guidelines and HIPAA regulations. Serum was grouped based on pathological grade: noncancer (three patients), low-risk cancer group (pT2a, Gleason 6, ISUP Grade Group 1; two patients), and high-risk cancer group (pT3, Gleason 8 or Gleason 9, ISUP Grade Group 4/5; two patients). A quality control (QC) human serum specimen representing a pool of 360 noncancer individuals was used as a control. Whole blood samples were initially collected in a serum vacutainer tube, centrifuged at 3000g for 15 min, and the collected serum was aliquoted and stored at −80 °C until profiled for miRNA expression. The 40% human serum was prepared by diluting 400 μL of QC serum in 600 μL of 1× PBS.

2.7. Serum Total RNA Isolation and qRT-PCR Detection of miRNAs. Total RNA was isolated from 350 mL of human serum (NC, LR, HR, QC) using a modified protocol for the miRNeasy Mini Kit (Qiagen). Specifically, 700 μL of QIAZol Lysis Reagent was added to the serum sample and incubated for 5 min at room temperature. Then, 140 μL of chloroform was added and mixed briefly and centrifuged for 15 min at 12 100 RPM at 4 °C. The upper aqueous layer was extracted and 1.5 volumes (1200 μL) of 100% ethanol was added and mixed. The sample was then loaded onto the miRNeasy mini column and the remaining protocol was followed. Total RNA was eluted with 50 μL of nuclease-free water, and 9.16 μL of eluted total RNA was used for each singleplex or multiplex reverse transcription and qRT-PCR reaction. MiRNA expression was verified using individual TaqMan-based qRT-PCR assays for *let*-7a and *let-7c* (Life Technologies; TaqMan Assay ID #000377, #000379, respectively). Reverse transcription reactions were performed on 9.16 μL of eluted total RNA with the TaqMan MicroRNA Reverse Transcription Kit and miRNA-specific stem-loop primers (Life Technologies) on a Applied Biosystems Veriti 96-well thermal cycler (Life Technologies) as previously described.[26] qRT-PCR reactions were prepared in triplicate; each reaction contains 1 μL of TaqMan real-time miRNA assay, 4.5 μL of reverse-transcribed RNA, 10 μL of TaqMan 2X Universal PCR Master Mix, No AmpErase UNG, and 4.5 μL of nuclease-free water. Real-time PCR reactions were run using an Applied Biosystems StepOnePlus Real-Time PCR System (Life Technologies) under the following conditions: 95 °C for 10 min, 40 cycles of 95 °C for 15 s, and 60 °C for 1 min. MiRNA expression was normalized to the endogenous serum reference gene miR-425-5p (Life Technologies; TaqMan Assay ID#001516) to obtain ΔCt values (Ct mir—Ct miR-425-5p) as previously described.[27] Average fold differences between noncancer (NC), low-risk (LR), and high-risk (HR) cancer serum relative to QC serum (representing pooled 360 noncancer patients) miRNA expression values were obtained using the ΔΔCt method.

https://doi.org/10.1021/acsomega.1c06479
ACS Omega 2022, 7, 2411−2418

3. RESULTS AND DISCUSSION

The potential clinical utility of miRNAs as biomarkers for cancers can provide a direct link to cancer diagnosis and prognosis as miRNAs are expressed in PCa cells and released into the surrounding biological fluids during disease progression. In biological fluids (e.g., serum), endogenous components such as proteins, cells, nucleotides, and pathogens have a propensity to strongly bind to the sensor's surface and thereby influence the performance accuracy (false-positive and false-negative responses) of diagnostic devices. In the present study, we determined if our improved plasmonic-based biosensor could detect miRNA levels with high sensitivity in a complex human fluid such as serum collected from the whole blood of noncancer and PCa patients. We previously identified a panel of PCa miRNA biomarkers (*let-7a, let-7c*, miR-141, miR-21, miR-200b) for the development of our nanoplsmonic TOF biosensor for PCa detection. Our previous studies revealed successful detection of miRNAs when diluted in a standard buffered solution using the functionalized AuTNPs-TOF-immobilized ssDNA/PEG-SH for hybridization with the synthetic target miRNA.[18] To prevent biofouling of the sensor surface, PEG_4-SH was grafted on AuTNPs as a spacer molecule to minimize nonspecific binding. In addition to its high water solubility and low toxicity, the combination of steric hindrance effects, chain length, grafting density, and chain conformation of PEG makes it an ideal antifouling molecule in biological environments. PEG grafting has been widely implemented as an antifouling polymer.[28]

Using the experimental setup described in Scheme 1, we measured miR-21 in diluted human QC serum (40% in PBS), representing a serum pool collected from 360 noncancer individuals. The $\Delta\lambda$peak was calculated as a function of time during target miR-21 hybridization with a ssDNA21-C3-SH:PEG-SH-functionalized AuTNPs-TOF plasmonic biosensor (Figure 1). An average $\Delta\lambda$peak red shift of 14.0 ± 0.8 nm

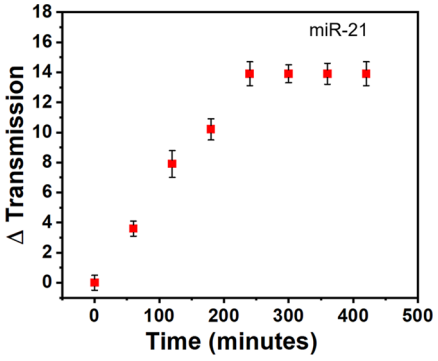

Figure 1. Change in transmission wavelength as a function of time during target miR-21 hybridization with ssDNA21-C3-SH:PEG-SH-functionalized AuTNPs-TOF with error bars (triplicates).

was observed after 4 h of hybridization followed by a plateau in the $\Delta\lambda$peak signal (Figure 1). The 4 h response time for ssDNA-miRNA hybridization enables the potential application of the TOF plasmonic biosensor in POC diagnosis. We then evaluated the linear response characteristics for a panel of PCa tumor suppressor and oncogenic miRNAs (*let-7a, let-7c*, miR-141, miR-21, miR-200b) using 40% human serum spiked with a predefined volume of 1 μM target miRNA to achieve a 1 fM−100 nM miRNA dilution curve in human serum. Eight hundred microliters of the miRNA-spiked serum solution was delivered to the biosensor for miRNA detection. The shift in transmission wavelength ($\Delta\lambda$) of the ssDNA/PEG thiol-fabricated AuTNPs laminated TOF plasmonic sensor upon hybridization of target miRNA in human serum in the range of 100 nM−1 fM was obtained. The sensor's sensitivity and limit of detection (LOD) along with the regression coefficient for each miRNA detected were calculated (Table 1).[25] The LODs

Table 1. AuTNP TOF Biosensor Regression Characteristics[25]

microRNA	sensitivity (nm/nM)	R^2	LOD (aM)
let-7a	1.0141	0.9761	394
miR-141	0.9026	0.9903	252
let-7c	0.9171	0.9817	242
miR-21	0.9084	0.9819	580
miR-200b	0.9714	0.9827	179

obtained for miR-200b, *let-7c*, miR-141, and *let-7a* were 179, 242, 252, and 394 aM, respectively, with a sensitivity ranging from 0.9714 to 1.0141 nm/nM. A slightly higher LOD of 580 was obtained for miR-21. The $\Delta\lambda_{peak}$ was observed to be correlated with miRNA concentration levels with a regression coefficient ranging from 0.9761 to 0.9903. These results exhibited improved LOD and sensitivity over our previously fabricated TOF plasmonic biosensor.[25]

To minimize the possibility of false-positive and false-negative responses, the selectivity characterization was performed using the complementary ssDNA probe to target miR-21 in 40% human serum. The spectrum obtained for the plasmonic sensor is shown in Figure 2 (green curve) with a

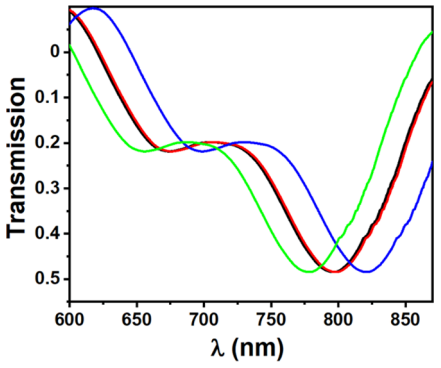

Figure 2. Transmission spectra demonstrating the selectivity of the fabricated TOF plasmonic biosensor. Green curve—AuTNP TOF plasmonic biosensor (776.8 nm), black curve—after immobilization of ssDNA21-C3-S-H: PEG4-SH (799 nm), red curve—after incubation in a solution mixture of microRNAs *let-7a, let-7c*, miR-200b, miR-141, and miR-21 (100 nM equimolar, 799.2 nm), and blue curve—after miR-21 hybridization (824.5 nm) in human serum.

λ_{peak} of 776.8 nm. Upon functionalization with the complementary ssDNA to target miR-21, the transmission peak red-shifted by 22.2−799 nm (black curve). The exposure of the ssDNA-functionalized biosensor to a solution mixture of 100 nM equimolar of miRNAs *let-7a, let-7c*, miR-200b, and miR-141 resulted in no significant shift in the $\Delta\lambda_{peak}$ (red curve overlapping black curve). Subsequently, the biosensor was incubated in 100 nM miR-21 in 40% human serum, which resulted in a 25.3 nm red shift in the λ_{peak} to 824.5 nm (blue curve). These results indicated high selectivity of the biosensor toward the target miRNA. We then validated the selective

https://doi.org/10.1021/acsomega.1c06479
ACS Omega 2022, 7, 2411−2418

binding of the target miRNA to the complementary ssDNA receptor in noncancer and cancer patient serums using the TOF plasmonic biosensor and qRT-PCR.

3.1. Detection of microRNAs in PCa Patient Samples.

The performance of the fabricated plasmonic biosensor was evaluated using seven human serum samples obtained from patients diagnosed with high-risk (HR), low-risk (LR) PCa and compared to noncancer (NC) patients. Two samples were obtained for each clinical PCa category, and three samples were obtained for noncancer controls. We tested if the plasmonic biosensor could be used to measure cancer-associated miRNAs in patient serums and differentiate between the clinical groups for PCa (Figure 3A–E). The levels of tumor suppressors miR-141, miR-200b, *let-7a*, and *let-7c* detected by the plasmonic biosensor were in the range of pM to fM in noncancer control serums and at lower concentrations in high-risk and low-risk patient samples. Figure 3A shows 110–290 fM, 18–28 fM, and 4–5 fM miR-141 in noncancer, low-risk, and high-risk patients, respectively. Likewise, low levels of miR-141 have been reported in the blood of PCa patients and function to block tumor growth and metastasis by targeting a cohort of pro-metastasis genes.[29,30]

Reduction of *let-7* family members such as *let-7a* and *let-7c* are commonly observed in PCa patients and in castration-resistant PCa (CRPC) cells.[31] They have been shown to inhibit PCa cell proliferation and clonal expansion *in vitro* and *in vivo*[28] by targeting cell cycle progression genes such as E2F2 and CCND2. The biosensor results revealed that *let-7a* is overall less abundant than *let-7c* and is expressed at the fM level, whereas *let-7c* is expressed at the pM level in human serum (Figure 3B,C). As expected, *let-7* levels were reduced in PCa cancer patients. For *let-7a*, noncancer serum levels were 58–90 fM, whereas low-risk and high-risk PCa serum levels dropped to 2–5 and 5–20 fM, respectively. Similar trends were noted for *let-7c*, and this miRNA was expressed at 0.8–1.2 pM in noncancer patient serum compared to 0.2–0.5 pM in low-risk and 0.4–0.5 pM in high-risk PCa serum.

In addition, miR-200b has also been identified as a PCa tumor suppressor miRNA that directly targets the androgen receptor and its expression is linked to decreased tumorigenicity and metastatic capacity of PCa cells.[32] Figure 3D shows miR-200b was expressed at 4–7, 0.1, and 0.1 pM in noncancer, low-risk, and high-risk patients, respectively. One-way ANOVA analysis showed that these tumor suppressor miRNAs (miR-141, miR-200b, *let-7a*, and *let-7c*) shown in Figure 3 offset panels could distinguish between the patient groups with high detection selectivity and a p-value <0.0001 for high-risk vs low-risk PCa patients. Figure 3E indicates that miR-21 expression was elevated in low-risk (4–5 pM) and high-risk (7–8 pM) patients compared to noncancer patients (0.3 pM). These findings are consistent with the oncogenic role for miR-21 to target and inhibit tumor suppressor gene PTEN expression and promote PCa cell proliferation and invasion.[33−36] miR-21 also showed a p-value <0.0001 for identification of noncancer control and high-risk vs low-risk patient groups.

Our data therefore indicated that the AuTNP-laminated TOF-based biosensor using serum expression profiles of these tumor suppressors and oncogenic-associated miRNAs could differentiate disease status. Indeed, the receiver operating characteristic (ROC) analysis shown in Figure 4 showed that the TOF plasmonic biosensor discriminated between the noncancer control group and the PCa groups (low-risk or

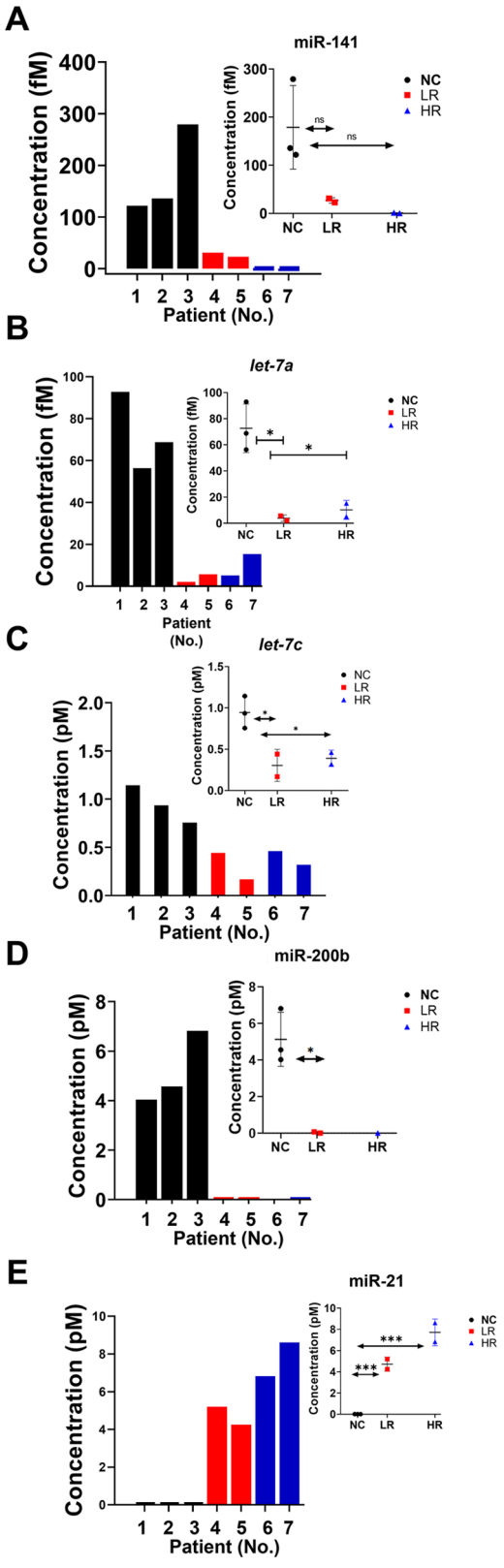

Figure 3. TOF plasmonic biosensor distinguishes the various clinical groups of PCa associated with miRNA. (A) 141, (B) *let-7a*, (C) *let-7c*, (D) miR-200b, and (E) miR-21 in noncancer (NC), low-risk (LR), and high-risk (HR) patients. Offset panels represent ANOVA results for NC vs LR vs HR samples. P (ns) = 0.1013, *P < 0.0159, and ***P < 0.0001 for NC and HR vs LR patients.

https://doi.org/10.1021/acsomega.1c06479
ACS Omega 2022, 7, 2411−2418

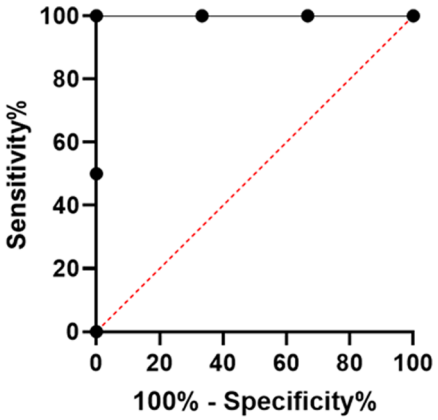

Figure 4. Receiver operating characteristics (ROC) for NC vs disease patient samples.

high-risk patients) with an area under the curve (AUC) of 1.0. This agreed with findings by Mitchell et al., where circulating miRNA-141 could discriminate PCa patients from noncancer patients.[37]

3.2. Relative Quantification of Serum miRNA Expression by qRT-PCR. We went on to examine two of the tumor suppressive miRNAs via conventional qRT-PCR methods for relative quantification analysis to compare miRNA expression profiles in noncancer, low-risk, and high-risk PCa patients from the same serum specimens used for the AuTNP-laminated TOF-based biosensor studies. Figure 5

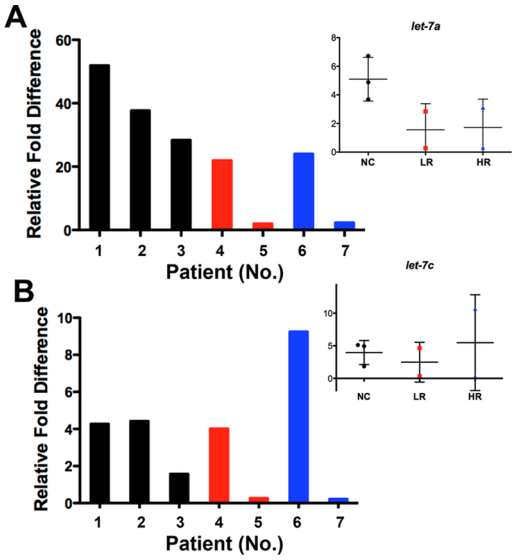

Figure 5. qRT-PCR of PCa-associated miRNAs. (A) *let-7a* and (B) *let-7c* in noncancer, low-risk, and high-risk patients. Offset panels represent ANOVA results for NC vs LR vs HR samples.

depicts the serum values obtained for *let-7a* and *let-7c* in the seven patients analyzed by TaqMan-based qRT-PCR. MiRNA expression for each individual patient serum was measured in triplicate relative to the miRNA expression profiled in the QC serum sample (representing pooled 360 noncancer patients), and the averaged fold differences were obtained using the comparative cycle threshold (ΔΔCt) method. Serum sample expression was normalized to the endogenous miRNA reference gene miR-425-5p.[20] Table 2 provides the mean serum values by qRT-PCR of tumor suppressors *let-7a* and *let-7c* for noncancer (NC), low-risk (LR), and high-risk (HR) patient groups, respectively. Our qRT-PCR analysis showed higher serum *let-7a* expression in noncancer individuals versus low-risk and high-risk PCa patients, which correlated with the results obtained using the TOF plasmonic biosensor. *let-7c* expression followed similar trends by qRT-PCR when comparing noncancer and low-risk patient groups; however, the large standard deviation for the high-risk group made this data point difficult to interpret. Larger clinical cohorts of human serum comparing miRNA expression levels using our biosensor and qRT-PCR are needed for further validation as well as the use of quantitative qRT-PCR rather than relative qRT-PCR methodologies.

Table 2. Relative miRNA Expression Using qRT-PCR (Mean ± SD)

miRNA	NC	LR	HR
let-7a	5.087 ± 1.529	1.562 ± 1.819	1.720 ± 1.982
let-7c	3.964 ± 1.846	2.488 ± 3.052	5.477 ± 7.342

Our study suggests that the use of miRNAs as biomarkers will provide tremendous opportunities for the development of point-of-care (POC) diagnostic tools to advance human health outcomes. To our knowledge, this study is the first to implement a TOF plasmonic biosensor for the detection of PCa miRNAs biomarkers. Furthermore, this work demonstrated that the TOF ssDNA-modified biosensor offers a highly selective receptor for the target miRNA detection for the early diagnosis of PCa directly from the patient's serum. Despite the limitation of a small patient cohort for this study, future studies building upon this work are envisioned to enable high-throughput miRNA assays on unmodified human fluids through the advancement of a sensor platform to a fully integrated microfluidic chip with multichannels for ultrasensitive quantification of miRNAs. Therefore, fabricated TOF plasmonic biosensors may have potential use for noninvasive miRNA diagnostic purposes in a large range of human disorders.

4. CONCLUSIONS

The AuTNP-laminated TOF plasmonic biosensor was successfully demonstrated using chemically synthesized plasmonic AuTNPs coupled with TOF to be a highly selective and specific miRNA assay in noncancer and PCa patient serums. A panel of miRNAs was quantified in human serum with a LOD in the aM range and a good miRNA hybridization response time of 4 h. As a proof-of-concept, the panel of miRNAs was assayed directly from the unmodified serum of seven patients with PCa. The biosensor demonstrated high specificity (p-value of <0.0001, AUC = 1.0) toward detection of the panel of miRNAs for early-stage diagnosis of PCa. The high specificity of fabricated biosensors may significantly advance the biosensing field by providing a POC tool to perform early-stage diagnosis and prognosis of diseases using miRNA or other biomarkers. The flexibility of this experimental setup has the potential to enable a wide range of POC applications for early disease diagnosis using miRNA-based biosensors as a promising noninvasive tool to diagnose PCa, where higher values on oncogenic and lower values of tumor suppressor miRNAs are significantly correlating with the presence of high-risk and metastatic disease. Although the panel of miRNAs was assayed using the fabricated biosensor to demonstrate proof-of-concept early-stage PCa diagnosis

https://doi.org/10.1021/acsomega.1c06479
ACS Omega 2022, 7, 2411−2418

toward improved health outcomes and patient survival rates, a larger cohort of PCa patients will need to be analyzed using this biosensor platform for biomarker validation.

AUTHOR INFORMATION

Corresponding Author

Gymama Slaughter − *Center for Bioelectronics, Bioelectronics Laboratory, Department of Electrical and Computer Engineering, Old Dominion University, Norfolk, Virginia 23508, United States;* orcid.org/0000-0002-4307-091X; Email: gslaught@odu.edu

Authors

Thakshila Liyanage − *Center for Bioelectronics, Bioelectronics Laboratory, Department of Electrical and Computer Engineering, Old Dominion University, Norfolk, Virginia 23508, United States*

Bayan Alharbi − *Center for Bioelectronics, Bioelectronics Laboratory, Department of Electrical and Computer Engineering, Old Dominion University, Norfolk, Virginia 23508, United States*

Linh Quan − *Leroy T. Canoles Jr. Cancer Research Center, Department of Microbiology and Molecular Cell Biology, Eastern Virginia Medical School, Norfolk, Virginia 23507, United States*

Aurora Esquela-Kerscher − *Leroy T. Canoles Jr. Cancer Research Center, Department of Microbiology and Molecular Cell Biology, Eastern Virginia Medical School, Norfolk, Virginia 23507, United States*

Complete contact information is available at: https://pubs.acs.org/10.1021/acsomega.1c06479

Author Contributions

G.S. conceived the project. T.L. and B.A. performed the biosensor experiment. T.L. analyzed the data and drafted the manuscript. G.S. revised the manuscript. A.E.-K. aided in miRNA gene selection for the study, defined the clinical cohorts to be compared, obtained the serum specimens from the EVMS biorepository, and edited the manuscript. A.E.-K. and L.Q. isolated RNA from the patients' serums and performed qRT-PCR validation studies and analyzed the data. All authors contributed to this work.

Notes

The authors declare no competing financial interest.

ACKNOWLEDGMENTS

This work was supported by National Science Foundation under Grant no. CBET-1921363 (to GS) and a Breedan Adams Foundation grant and a Commonwealth Health Research Board grant under award no. CHRB-274-11-20 (to AEK).

REFERENCES

(1) Bray, F.; Ferlay, J.; Soerjomataram, I.; Siegel Rebecca, L.; Torre Lindsey, A.; Jemal, A. Global cancer statistics 2018: GLOBOCAN estimates of incidence and mortality worldwide for 36 cancers in 185 countries. *Ca-Cancer J. Clin.* **2018**, *68*, 394−424.

(2) Rawla, P. Epidemiology of prostate cancer. *World J. Oncol.* **2019**, *10*, 63−89.

(3) Humphrey, P. A. Histopathology of prostate cancer. *Cold Spring Harbor Perspect. Med.* **2017**, *7*, No. a030411.

(4) Descotes, J.-L. Diagnosis of prostate cancer. *Asian J. Urol.* **2019**, *6*, 129−136.

(5) Cuzick, J.; Thorat Mangesh, A.; Andriole, G.; Brawley Otis, W.; Brown Powel, H.; Culig, Z.; Eeles Rosalind, A.; Ford Leslie, G.; Minasian Lori, M.; Hamdy Freddie, C.; Holmberg, L.; Ilic, D.; Key Timothy, J.; La Vecchia, C.; Lilja, H.; Marberger, M.; Meyskens Frank, L.; Parker, C.; Parnes Howard, L.; Perner, S.; Rittenhouse, H.; Schalken, J.; Schmid, H.-P.; Schmitz-Drager Bernd, J.; Schroder Fritz, H.; Stenzl, A.; Tombal, B.; Wilt Timothy, J.; Wolk, A. Prevention and early detection of prostate cancer. *Lancet Oncol.* **2014**, *15*, e484−492.

(6) Tobore, T. O. On the need for the development of a cancer early detection, diagnostic, prognosis, and treatment response system. *Future Sci. OA* **2020**, *6*, No. FSO439.

(7) Condrat, C. E.; Thompson, D. C.; Barbu, M. G.; Bugnar, O. L.; Boboc, A.; Cretoiu, D.; Suciu, N.; Cretoiu, S. M.; Voinea, S. C. miRNAs as biomarkers in disease: latest findings regarding their role in diagnosis and prognosis. *Cells.* **2020**, *9*, No. 276.

(8) Pal, M. K.; Jaiswar, S. P.; Dwivedi, V. N.; Tripathi, A. K.; Dwivedi, A.; Sankhwar, P. MicroRNA: a new and promising potential biomarker for diagnosis and prognosis of ovarian cancer. *Cancer Biol. Med.* **2015**, *12*, 328−341.

(9) Joshi, G. K.; Deitz-McElyea, S.; Liyanage, T.; Lawrence, K.; Mali, S.; Sardar, R.; Korc, M. Label-free nanoplasmonic-based short noncoding RNA sensing at attomolar concentrations allows for quantitative and highly specific assay of MicroRNA-10b in biological fluids and circulating exosomes. *ACS Nano* **2015**, *9*, 11075−11089.

(10) Liyanage, T.; Masterson, A. N.; Oyem, H. H.; Kaimakliotis, H.; Nguyen, H.; Sardar, R. Plasmoelectronic-Based Ultrasensitive Assay of Tumor Suppressor microRNAs Directly in Patient Plasma: Design of Highly Specific Early Cancer Diagnostic Technology. *Anal. Chem.* **2019**, *91*, 1894−1903.

(11) Masterson, A. N.; Liyanage, T.; Berman, C.; Kaimakliotis, H.; Johnson, M.; Sardar, R. A novel liquid biopsy-based approach for highly specific cancer diagnostics: mitigating false responses in assaying patient plasma-derived circulating microRNAs through combined SERS and plasmon-enhanced fluorescence analyses. *Analyst* **2020**, *145*, 4173−4180.

(12) Masterson, A. N.; Liyanage, T.; Kaimakliotis, H.; Gholami Derami, H.; Deiss, F.; Sardar, R. Bottom-Up Fabrication of Plasmonic Nanoantenna-Based High-throughput Multiplexing Biosensors for Ultrasensitive Detection of microRNAs Directly from Cancer Patients' Plasma. *Anal. Chem.* **2020**, *92*, 9295−9304.

(13) Zhang, L.; Xu, Y.; Jin, X.; Wang, Z.; Wu, Y.; Zhao, D.; Chen, G.; Li, D.; Wang, X.; Cao, H.; Xie, Y.; Liang, Z. A circulating miRNA signature as a diagnostic biomarker for non-invasive early detection of breast cancer. *Breast Cancer Res. Treat* **2015**, *154*, 423−434.

(14) Esquela-Kerscher, A.; Slack, F. J. Oncomirs - microRNAs with a role in cancer. *Nat. Rev. Cancer* **2006**, *6*, 259−269.

(15) Rufino-Paiomares, E. E.; Reyes-Zurita, F. J.; Lupianez, J. A.; Medina, P. P. MicroRNAs as Oncogenes and Tumor Suppressors. *MicroRNAs in Medicine*; John Wiley & Sons, Inc., 2014; pp 223−243.

(16) Hasegawa, T.; Lewis, H.; Esquela-Kerscher, A. The role of non-coding RNAs in prostate cancer. In *Translating MicroRNAs to the Clinic.*; Laurence, J., Ed.; Elsevier Inc., 2017; pp 329−369.

(17) Samarah, L. Z.; Vertes, A. Mass spectrometry imaging based on laser desorption ionization from inorganic and nanophotonic platforms. *View* **2020**, *1*, No. 20200063.

(18) Cao, J.; Shi, X.; Gurav, D. D.; Huang, L.; Su, H.; Li, K.; Niu, J.; Zhang, M.; Wang, Q.; Jiang, M.; Qian, K. Metabolic fingerprinting on synthetic alloys for medulloblastoma diagnosis and radiotherapy evaluation. *Adv. Mater.* **2020**, *32*, No. 2000906.

(19) Pei, C.; Liu, C.; Wang, Y.; Cheng, D.; Li, R.; Shu, W.; Zhang, C.; Hu, W.; Jin, A.; Yang, Y.; Wan, J. FeOOH@ metal−organic framework core−satellite nanocomposites for the serum metabolic fingerprinting of gynecological cancers. *Angew. Chem., Int. Ed.* **2020**, *59*, 10831−10835.

(20) Lai, M.; Slaughter, G. Label-free MicroRNA optical biosensors. *Nanomaterials* **2019**, *9*, No. 1573.

(21) Slaughter, G. Current advances in biosensor design and fabrication. *Encyclopedia of Analytical Chemistry: Applications, Theory and Instrumentation* **2006**, *15*, 1−25.

(22) Zhou, L.; Liu, Y.; Wang, F.; Jia, Z.; Zhou, J.; Jiang, T.; Petti, L.; Chen, Y.; Xiong, Q.; Wang, X. Classification analyses for prostate cancer, benign prostate hyperplasia and healthy subjects by SERS-based immunoassay of multiple tumour markers. *Talanta* **2018**, *188*, 238−244.
(23) Liu, J.; Cai, C.; Wang, Y.; Liu, Y.; Huang, L.; Tian, T.; Yao, Y.; Wei, J.; Chen, R.; Zhang, K.; Liu, B.; et al. A biomimetic plasmonic nanoreactor for reliable metabolite detection. *Adv Sci.* **2020**, *7*, No. 1903730.
(24) Zhang, Y.; Zhang, X.; Situ, B.; Luo, S.; Wu, Y.; Zheng, L.; Qiu, Y. Rapid electrochemical biosensor for sensitive profiling of exosomal microRNA based on multifunctional DNA tetrahedron assisted catalytic hairpin assembly. *Biosens. Bioelectron.* **2021**, *183*, No. 113205.
(25) Liyanage, T.; Lai, M.; Slaughter, G. Label-free tapered optical fiber plasmonic biosensor. *Anal. Chim. Acta* **2021**, *1169*, No. 338629.
(26) Lewis, H.; Lance, R.; Troyer, D.; Beydoun, H.; Hadley, M.; Orians, J.; et al. miR-888 is an expressed prostatic secretions-derived microRNA that promotes prostate cell growth and migration. *Cell Cycle* **2014**, *13*, 227−239.
(27) Joshi, G. K.; Deitz-McElyea, S.; Johnson, M.; Mali, S.; Korc, M.; Sardar, R. Highly specific plasmonic biosensors for ultrasensitive microRNA detection in plasma from pancreatic cancer patients. *Nano Lett.* **2014**, *14*, 6955−6963.
(28) Chu, M. K.; Gordijo, C. R.; Li, J.; Abbasi, A. Z.; Giacca, A.; Plettenburg, O.; Wu, X. Y. In vivo performance and biocompatibility of a subcutaneous implant for real-time glucose-responsive insulin delivery. *Diabetes Technol. Ther.* **2015**, *17*, 255−267.
(29) Kumar, B.; Rosenberg, A. Z.; Choi, S. M.; Fox-Talbot, K.; De Marzo, A. M.; Nonn, L.; Brennen, W. N.; Marchionni, L.; Halushka, M. K.; Lupold, S. E. Cell-type specific expression of oncogenic and tumor suppressive microRNAs in the human prostate and prostate cancer. *Annu. Rev. Cancer Biol.* **2018**, *8*, No. 7189.
(30) Nadiminty, N.; Tummala, R.; Lou, W.; Zhu, Y.; Shi, X.-B.; Zou, J. X.; Chen, H.; Zhang, J.; Chen, X.; Luo, J.; de Vere White, R. W.; Kung, H.-J.; Evans, C. P.; Gao, A. C. MicroRNA let-7c is downregulated in prostate cancer and suppresses prostate cancer growth. *PLoS One* **2012**, *7*, No. e32832.
(31) Dong, Q.; Meng, P.; Wang, T.; Qin, W.; Qin, W.; Wang, F.; Yuan, J.; Chen, Z.; Yang, A.; Wang, H. MicroRNA let-7a inhibits proliferation of human prostate cancer cells in vitro and in vivo by targeting E2F2 and CCND2. *PLoS One* **2010**, *5*, No. e10147.
(32) Williams, L. V.; Veliceasa, D.; Vinokour, E.; Volpert, O. V. miR-200b inhibits prostate cancer EMT, growth and metastasis. *PLoS One* **2013**, *8*, No. e83991.
(33) Yang, Y.; Guo, J.-X.; Shao, Z.-Q. miR-21 targets and inhibits tumor suppressor gene PTEN to promote prostate cancer cell proliferation and invasion: An experimental study. *Asian Pac. J. Trop. Med.* **2017**, *10*, 87−91.
(34) Folini, M.; Gandellini, P.; Longoni, N.; Profumo, V.; Callari, M.; Pennati, M.; Colecchia, M.; Supino, R.; Veneroni, S.; Salvioni, R.; Valdagni, R.; Daidone, M. G.; Zaffaroni, N. miR-21: an oncomir on strike in prostate cancer. *Mol. Cancer* **2010**, *9*, No. 12.
(35) Feng, Y.-H.; Tsao, C.-J. Emerging role of microRNA-21. *Biomed. Rep.* **2016**, *5*, 395−402.
(36) Ribas, J.; Ni, X.; Haffner, M.; Wentzel, E. A.; Salmasi, A. H.; Chowdhury, W. H.; Kudrolli, T. A.; Yegnasubramanian, S.; Luo, J.; Rodriguez, R.; Mendell, J. T.; Lupold, S. E. miR-21: An Androgen Receptor-Regulated MicroRNA that Promotes Hormone-Dependent and Hormone-Independent Prostate Cancer Growth. *Cancer Res.* **2009**, *69*, 7165−7169.
(37) Mitchell, P. S.; Parkin, R. K.; Kroh, E. M.; Fritz, B. R.; Wyman, S. K.; Pogosova-Agadjanyan, E. L.; et al. Circulating microRNAs as stable blood-based markers for cancer detection. *Proc. Natl. Acad. Sci. U.S.A.* **2008**, *105*, 10513−10518.

https://doi.org/10.1021/acsomega.1c06479
ACS Omega 2022, 7, 2411−2418